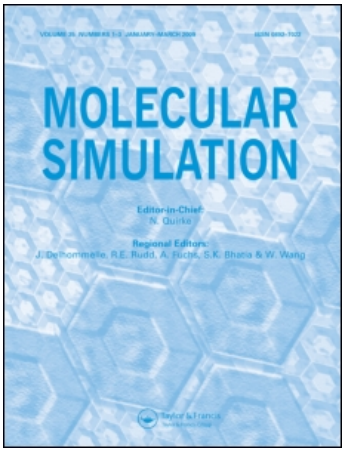

Molecular Simulation
Publication details, including instructions for authors and subscription information:
http://www.informaworld.com/smpp/title~content=t713644482

Picosecond Laser Processing of Copper and Gold

Clifton F. Richardson[a]; Paulette Clancy[a]
[a] Cornell School of Chemical Engineering, University, Ithaca, NY, USA

To cite this Article Richardson, Clifton F. and Clancy, Paulette(1991) 'Picosecond Laser Processing of Copper and Gold', Molecular Simulation, 7: 5, 335 — 355
To link to this Article: DOI: 10.1080/08927029108022461
URL: http://dx.doi.org/10.1080/08927029108022461

Molecular Simulation, 1991, Vol. 7, pp. 335–355
Reprints available directly from the publisher
Photocopying permitted by license only

PICOSECOND LASER PROCESSING OF COPPER AND GOLD: A COMPUTER SIMULATION STUDY

CLIFTON F. RICHARDSON and PAULETTE CLANCY*

School of Chemical Engineering, Cornell University, Ithaca, NY 14853, USA

(Received February 1991, accepted April 1991)

Non-equilibrium Molecular Dynamics Simulation methods have been used to study the ability of Embedded Atom Method models of the metals copper and gold to reproduce the equilibrium and non-equilibrium behavior of metals at a stationary and at a moving solid/liquid interface. The equilibrium solid/vapor interface was shown to display a simple termination of the bulk until the temperature of the solid reaches $\approx 90\%$ of the bulk melting point. At and above such temperatures the systems exhibit a surface disordering known as surface melting. Non-equilibrium simulations emulating the action of a picosecond laser on the metal were performed to determine the regrowth velocity. For copper, the action of a 20 ps laser with an absorbed energy of 2–5 mJ/cm^2 produced a regrowth velocity of 83–100 m/s, in reasonable agreement with the value obtained by experiment (> 60 m/s). For gold, similar conditions produced a slower regrowth velocity of 63 m/s at an absorbed energy of 5 mJ/cm^2. This is almost a factor of two too low in comparison to experiment (> 100 m/s). The regrowth velocities of the metals seems unexpectedly close to experiment considering that the free-electron contribution is ignored in the Embeeded Atom Method models used.

KEY WORDS: Non-equilibrium computer simulation, molecular dynamics, crystal growth, Embedded Atom Method models of metals.

1 INTRODUCTION

Rapid solidification processes are of increasing importance in the production of metastable new alloys involving metals, ceramics and composites. In this paper we shall present non-equilibrium Molecular Dynamics (NEMD) simulations of the rapid solidification of metals. Earlier, we developed an NEMD method suitable for the study of ultra-rapid melting and resolidification processes and tested its qualitatively predictive capabilities using a simple Lennard–Jones system [1]. However, a quantitative comparison was not possible since the Lennard–Jones potential is not a good model for the experimental system considered, silicon, and because the experimental conditions, involving a 2 ns pulse, could not be duplicated. Since then McDonald *et al.* [2] have reported the results of pulsed irradiation of the noble metals copper and gold using a picosecond laser. This presents the first opportunity for the NEMD method to be applied to systems for which good interatomic force models are available (i.e. which reproduce well the solid properties of the materials) as well as involving conditions of pulse duration (20 ps) and absorbed energy fluence (5 mJ cm^{-2}) which can be applied in the simulation. McDonald *et al.* report very high resolidification velocities for these models (> 60 m s^{-1} for copper and > 100 m s^{-1} for gold). At comparable fractions of the bulk melting temperature, such velocities are

*Author to whom correspondence should be addressed.

higher than either non-metallic systems, such as Lennard-Jones atoms [1], or semiconductors (as modelled, for example, by the Stillinger-Weber model [3] or from experimental measurements for silicon [4]). It will be interesting to discover whether a model such as EAM which ignores the free electron contribution to the transport properties (a dominant contribution for metals) can still produce quantitatively accurate regrowth velocities.

The organization of this paper is as follows: section 2 gives a brief description of the NEMD method; section 3 describes results for the rapid solidification of copper together with studies of the equilibrium crystal/vapor interface; section 4 reports studies of an EAM model of gold and section 5 summarizes our findings.

2 NON-EQUILIBRIUM COMPUTER SIMULATION METHOD

2.1 Simulation Cell and Material Preparation

The configuration for the simulation cell used in our studies is shown schematically in Figure 1. The "dynamic solid" region of the cell is composed of a substrate of N atoms modelled using the Embedded Atom Method (EAM) reviewed briefly in section 2.2. In order to verify our EAM code we compared the density produced in an isothermal-isobaric (NPT) simulation at zero pressure against Foiles *et al.*'s results for a liquid state point for Cu and Au [9] and found in all cases that the density was within 1% of their results. The lattice constant in our simulation was within 2% of the experimental value and within 0.5% of that given by Foiles *et al.* In order to prepare a solid/vapor interface, we first ran a Molecular Dynamics simulation employing an isobaric-isothermal ensemble (constant number of atoms, pressure and temperature) for the bulk solid for around 25,000 time steps in order for the system to come to configurational equilibrium. Following this, a vapor is created above the

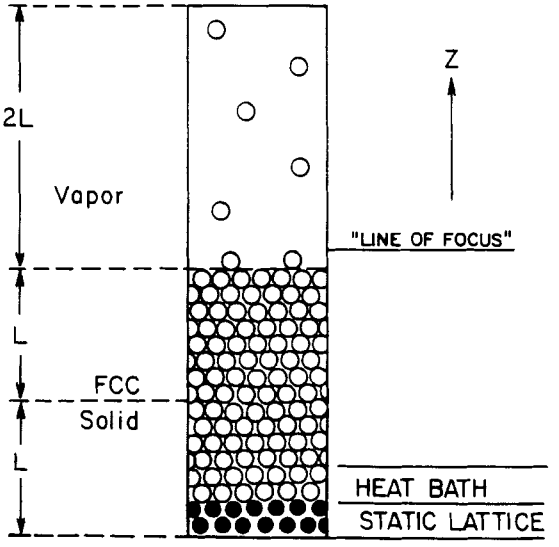

Figure 1 Schematic diagram of the simulation cell showing the original solid/vapor interface of the system and the location of the heat bath and fixed lattice regions.

Table 1 Two-dimensional structure factors for EAM copper at 1253.5 K.

*Layer Number**	$\|S(k)\|^{2\dagger}$
1	0.0009
2	−0.0994
3	0.1653
4	0.4896
5	0.707

*Numbers increase from the topmost layer down.
†A two-dimensional structure factor, $|S(k)|^2$, value of zero indicates a randomly structured (liquid-like) 2-D plane. A value of unity shows perfect ordering (crystalline). This structure is defined as Re $S(k) \equiv$ Re $[e^{ikr}]$.

solid and several layers of atoms at the bottom of the underlying substrate (four say, depending on the range of the potential) are fixed on lattice sites. A heat sink, consisting of a further three atomic planes, is employed to emulate the presence of an underlying depth of substrate. In this region, the velocities of the particles are rescaled to maintain the substrate temperature. This configuration is then equilibrated further (for 45,000 time steps usually) until configurational equilibrium has again been attained. A by-product of this material preparation stage is that analysis of the atomic positions (via structure factors and computer graphics) can readily show the presence, if any, of surface melting (a wetting phenomenon) at a given temperature. We shall report here to what extent EAM metals exhibit surface melting. At lower temperatures, the interlayer spacing close to the vapor interface is investigated since metals and non-metals show a differing spacing close to the vapor interface.

From past experience we have found it necessary for the system to contain at least 4,000 and, preferably, 8,000 particles in non-equilibrium simulations of solidification [1,6]. Such a system size helps to improve statistics, reduce the effect of the periodic boundary conditions and to distance the heat bath from the portion of substrate affected by the 'laser'. The system size must be sufficiently large for the interface temperature to reach a constant undercooling during the period of steady-state crystallization. The 4096 atom system used for most of the simulations has 25 layers of atoms above the heat bath, with 128 atoms per layer. The 8072 atom system also used here has twice the number of layers but the same number of atoms per layer. The simulation cell is thus a 2 × 1 × 1 parallelopiped (i.e. "brick" shaped) for the 4096-atom system and a 4 × 1 × 1 parallelopiped for the larger system.

For the simulation cell shown in Figure 1, we select a substrate temperature which is maintained with the aid of the heat bath. We also select the orientation of the crystal lattice (here, the exposed face is (100)) and choose an appropriate energy fluence and pulse duration. Here, where our aim is to duplicate experimental results, we have used a 20 ps pulse and a fluence which results in an absorbed energy of 1–3.2 mJ cm^{-2} (the absorbed energy found experimentally for gold is 5 mJ cm^{-2}). The effect of changing the pulse duration is also investigated. This pulse duration and energy input causes up to half the 4096-atom system to melt. Thus the conditions of our simulation closely emulate experimental conditions. We are able to predict the overheating and undercooling arising from the simulation of the physical set-up and processing conditions. We are also able to study in one simulation run both the melting and resolidification processes as they occur, whereas most other simulation studies focus on the resolidification alone.

2.2 *Interatomic Potential Models for Metals*

The Embedded Atom Method developed by Daw, Baskes and Foiles at Sandia has gained prominence for the calculation of the properties of metals and alloys [7–9]. Finnis and Sinclair have an analogous model [10], also based on a tight-binding model. The Embedded Atom Method involves a many-body potential derived from density functional theory. The total internal energy of the system, E_{tot}, is a sum over all atoms i,

$$E_{tot} = \sum_i E_i \tag{1}$$

The energy associated with each atom is split into two terms, (i) the energy required to embed an atom into the electron density associated with the host (i.e. the other atoms in the system) and (ii) a repulsive core interaction. Thus

$$E_i = \sum_i F_i(\rho_{h,i}) + \frac{1}{2} \sum_{\substack{i,j \\ j \neq i}} \phi_{ij}(r_{ij}) \tag{2}$$

where F_i is the embedding energy of atom i, $\rho_{h,i}$ is the electron density of the host at the position of atom i, ϕ_{ij} is the repulsive pair potential and r_{ij} is the interatomic separation of atoms i and j. The electron density of the host is approximated by a superposition of atomic electron densities as:

$$\rho_{h,i} = \sum_{j \neq i} \rho_j^a(r_{ij}) \tag{3}$$

where $\rho_j^a(r_{ij})$ is the electron density at r_{ij} due to j. This allows the force on atom i to be given by

$$F_i = -\nabla_{r_i} E_i = -\sum_{j \neq i} \left[\frac{\partial F_i}{\partial \rho_j^a} \frac{d\rho_j^a}{dr_{ij}} + \frac{\partial F_j}{\partial \rho_i^a} \frac{d\rho_i^a}{dr_{ij}} + \frac{d\Phi_{ij}}{dr_{ij}} \right] \frac{r_{ij}}{|r_{ij}|} \tag{4}$$

Oh and Johnson have presented an alternative, simplified EAM description and parameters for fcc, hcpa nd bcc metals [11,12] and a simple prescription for binary alloys [13]. In Oh and Johnson's approach, the electron density is an empirically-determined, exponentially-decaying function. The embedding function for both the Foiles et al. and Oh and Johnson methods is given by

$$F_i(\rho_{h,i}) = E - \frac{1}{2} \sum_{j \neq i} \phi_{ij}(r_{ij}) \tag{5}$$

although the form of E_i is obtained from different sources in the two formulations. Since the argument of $F_i(\rho_{h,i})$ is a sum of pairwise-additive quantities and ϕ_{ij} is also pairwise-additive, the EAM potential does not require an enormous increase in computational resources. The computational effort involved in an EAM model is a factor of five more than that for Lennard–Jones atoms but the reduced time step for copper is 2.4 times as big as LJ, thus the overall computational speed of an EAM simulation is roughly twice as slow as that for a Lennard–Jones system. The time steps for copper and gold are 4.50 and 7.05 fs respectively; these values were found to give good energy conservation over 50,000 time steps for 4096 atoms. On the Cornell National Supercomputer Facility's IBM 3090-600 J machine, the unvectorized EAM code produced 1200 time steps per CPU hour for a system of 4096 atoms.

2.3 Non-Equilibrium Molecular Dynamics Method

A thermal gradient is introduced into the system by depositing energy via so-called "energy carriers". A chosen energy fluence, scaled to the microscopic size of the simulation cell, is divided equally among these carriers which appear to be atoms with momentum but no volume and virtually no mass (i.e. a crude model for a photon). The carriers collide with the solid substrate, transfer some of this energy and disappear. The number of energy carriers is set to 45% of the number of atoms following the studies made in [1]. Depending on the fluence, substrate temperature etc., this may cause part of the system to melt. As the system melts, some atoms will now lie above the line of focus shown in Figure 1. While they remain above this line they do not contribute to the energy transfer process. This accounts in a simple way for the change in reflectivity on melting. A short while after the energy input ceases, the solid/liquid interface halts its progression into the substrate and then regrows as a solid (usually crystalline, unless the resolidification velocity is too fast).

The main tasks for the non-equilibrium simulation program are to locate the rapidly moving solid/liquid interface, to evaluate the diffusivity of each "layer" and to monitor thermodynamic properties (such as the interface temperature), structural properties (locations of vacancies and interstitials) and kinetic properties (e.g. interface velocity) each as a function of time. Of particular importance here, the velocity and temperature of the interface can readily be calculated as a function of time (see [1] for example). These properties both show a period of constancy, signalling the period of steady-state recrystallization. The steady-state regrowth velocity changes in response to a change in the substrate temperature, i.e. that maintained by the heat bath in our simulation: the interface velocity will increase as the substrate temperature is lowered (i.e. the undercooling is increased). A number of simulations were performed with different substrate temperatures in order to produce different interface velocities.

The NEMD method used here was shown to be capable of locating the extent of the diffuse transient solid/liquid interface for Lennard–Jones particles with a temporal and spatial resolution of 1–5 ps and 3.0 Å respectively. This is achieved by investigation of the two-dimensional density profiles and layer-wise radial distribution functions, $g(r)$. A layer is approximately one atomic diameter thick (i.e. it encompasses one lattice plane in the solid; the definition of a layer in a liquid is somewhat arbitrary). The last point (height within the box, z) at which crystalline behavior is exhibited and the point marking the onset of fully liquid behavior are found from both properties and define the extent of the interface. An analysis of in-plane diffusion coefficients, order parameters and computer graphics views of each layer are used to refine and corroborate these results. This is the most time-consuming part of the post-simulation analysis.

Knowledge of the interface position as a function of time serves as the starting point for the calculation of other properties such as the interface velocity and temperature. The slope of the melt depth-time curve gives the interface velocity. The velocity is most accurately determined during the resolidification regime and least accurately determined during the transition from the very rapid "melt-in" regime to the resolidification regime (i.e., around the point where the velocity is zero). This is unfortunate since the zero velocity point is of importance both as a route to the bulk melting point and for the investigation of any asymmetry which may occur between the kinetics of melting and freezing. Again, knowing the location of the interface as a function of

time we can calculate the kinetic energy of the particles in the interfacial region and hence obtain the temperature of the interface as a function of time. Calculation of the interface velocity, v, and interface temperature, T, allows the construction of the interface response function, v–T, which provides information regarding the kinetics of rapid melting and resolidification. We also use the interface response function as a route to the determination of the melting point: the temperature at which the velocity of the interface is zero corresponds to the bulk melting point of the material. For EAM metals, we estimate the accuracy of this method to determine the melting point to be 5%.

3 RESULTS FOR EAM COPPER

We chose to study the results of "irradiating" copper with the substrate held at three different temperatures: T_{subs} = 300, 710, 1236 K. Once we established the bulk melting point, T_m, of the EAM model from the interface response function, these temperatures were found to correspond to 22%, 53% and 92% of T_m. The first of these temperatures, 300 K, corresponds to the temperature at which the experiments of McDonald *et al.* [2] were performed. The second temperature was chosen so that we could compare the interface morphology and resolidification velocity for EAM metals to our earlier results for Lennard–Jones atoms [1] at an equivalent position in the phase diagram, chosen here to be the same fraction of the melting point. The third temperature was again chosen to be equivalent to an earlier LJ run, one at which surface melting had been observed [14]. For each of these temperatures we observed the state of the equilibrium solid/vapor interface at the end of the NVT equilibration period and then subjected the solid to "irradiation" by a 20 ps "laser" pulse and followed the subsequent melting and resolidification. The results are now given for each investigation. The EAM model chosen for copper was that due to Foiles [9].

3.1 The Equilibrium Solid/Vapor Interface

At the two lower temperatures, the equilibrium solid/vapor interface is characterized by a simple termination of the bulk. However, inspection of the interplanar spacing between the topmost two layers at 300 K showed a 6% contraction, with a very small contraction (0.5%) between layers 2 and 3. These results compare favorably with the ion beam scattering results of Haberle and Gustafsson [15], where a 7.5% contraction was found between layers 1 and 2 followed by a 2.5% expansion between layers 2 and 3. It should be noted, for comparison, that a simple pair potential such as a Lennard-Jones potential shows a 7% expansion between layers 1 and 2 at an equivalent temperature, while a Stillinger-Weber model of silicon shows a 12% contraction [16]. Thus the contraction observed for copper appears to be evidence that the potential model is reasonably appropriate in reproducing the structure of the metallic crystal/vapor interface. This is interesting as the surface represents a very different situation from that under which the potential parameters were fitted.

At 0.92 T_m, there is evidence from the two-dimensional layerwise order parameters (see Table 1), diffusion coefficients and from a computer graphics analysis that the top three or four layers of the metal are disordered, with liquid-like diffusion coefficients and a pronounced lack of structure. For comparison, a Lennard-Jones system of atoms at a T_{subs}/T_m value of 0.95 showed only one layer of atoms with a disordered,

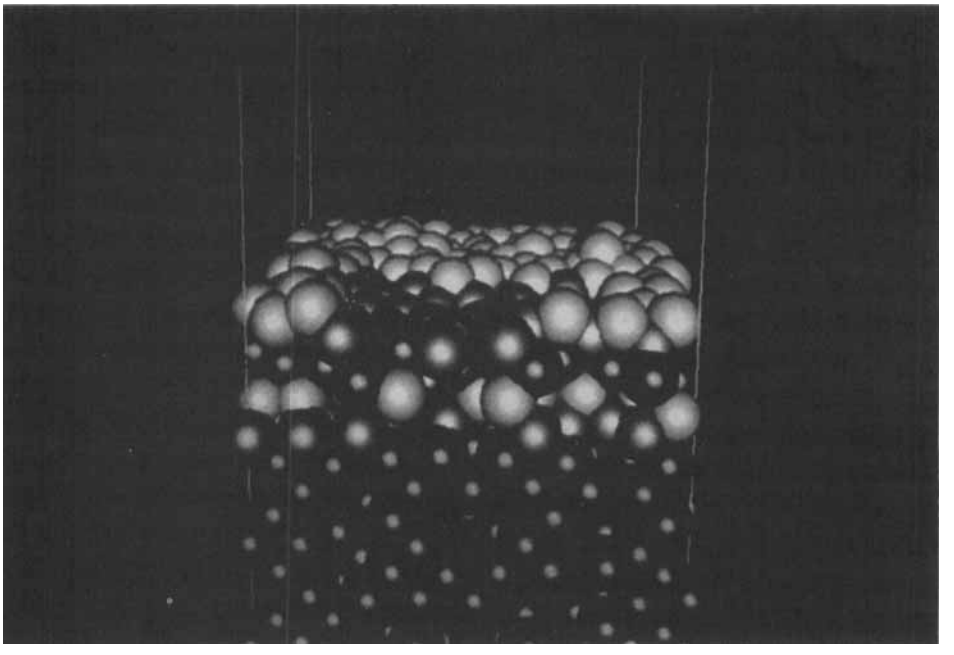

Figure 2 Computer graphics-derived photograph of the uppermost layers of the surface of EAM copper. Here the top layer contains an incomplete number of atoms for a full plane (in fact, here it is half empty). A reconstruction of the surface appears as a 'wave' in the top 2–3 layers of the system which is absent in a system where the top layer contains a complete number of atoms. The key to the layers is red for the top layer, green for the next layer and blue for the next layer. Note that apparent gaps in the solid are caused by the location of the periodic boundary conditions (See color plate I).

liquid-like structure. Thus the surface melting of an EAM metal is significantly more than for a typical non-metal under comparable conditions, in line with experimental observation. Surface melting has been observed experimentally, for example, for lead crystals [17] and films [18] and for films of neon and argon [19].

We have also noticed an interesting feature of this surface-melted layer. When the top layer contains a full complement of atoms, the disordered layer shows complete randomness with no discernible difference in z-value. However, if the top layer of atoms forms an incomplete plane (in our case equivalent to a 0.50 monolayer coverage) there appears to be a structural change in the top two layers reminiscent of a corrugation (see Figure 2). Analysis of the z-values of neighboring atoms shows that there is a sinusoidal-like correlation between them, forming a repeating pattern involving ten atoms. Such a phenomenon has been seen experimentally in adatom-induced reconstruction. Close-packed (111) faces of gold show a surface reconstruction with a repeating periodicity pattern every 22 atoms [20]. Equilibrium Molecular Dynamics simulations have studied this reconstruction [21,22] at a defect-free (111) crystal/vapor interface (i.e. well below the onset of surface melting) using a "glue potential" [23] which is similar to an EAM model. The observed reconstruction in the simulated system had a repeating pattern every 11 atoms, i.e. half the experimental unit cell. However, our observations are the first simulation evidence for adatom-induced reconstruction in metals. We are now investigating this phenomenon further.

3.2 *Rapid Melting and Resolidification of EAM Copper*

Systems of 4096 and 8072 atoms of EAM copper were equilibrated, as described earlier, with the substrate held at three different temperatures and then melted using various laser fluences and pulse durations. This allowed us to determine the effect of both fluence and pulse duration on the resolidification characteristics. It should be noted that the larger 8072-atom system was studied at 300 K only, for comparison with experiment.

Morphology of the interface

Inspection of the density profile of the sytem, the two-dimensional $g(r)$, order parameters and in-plane diffusion coefficients, in short the information we use to locate the interface, gives a good description of the morphology of the interface. We found that the solid/liquid interface existing during rapid melting and resolidification was diffuse, as Chen *et al.* had observed for the equilibrium solid/liquid interface of EAM nickel [24]. The extent of the interface encompassed, on average, three atomic layers with a gradual transition from crystalline to liquid character. The interface was somewhat wider during the "melt-in" part of the simulation, being 4 or 5 layers wide. For the results at 710 K and 1236 K ($T/T_m = 0.53$ and 0.92 respectively) we can compare the morphology of the interface to that for a system of Lennard-Jones (LJ) atoms. We were somewhat surprised to find that the EAM interface was less diffuse than that for the Lennard-Jones: at 710 K the average width of the EAM interface was three layers, whereas the LJ interface was five layers wide. We had anticipated that the nearly free electron distribution in metals and the, not unassociated, small volume change on melting would result in a somewhat more diffuse solid/liquid interface. This is apparently not the case, at least within the framework of an EAM model for metals. This observation of the relative diffuseness of EAM and LJ models was also found at the highest temperature studied, 1236 K.

Effect of laser fluence and pulse duration

NEMD simulation runs were performed in which the energy absorbed by the EAM copper atoms was 3.20, 2.45, 2.03 and 1.86 mJ cm^{-2}. The resulting melt depth versus time, interface velocity versus time, interface temperature versus time and interface response functions were evaluated for each simulation, as described in section 2.3. A representative set of these results is shown in Figures 3–6 for a pulse duration of 20 ps and an absorbed fluence of 2.03 mJ/cm^2. The melt depth versus time curve shown in Figure 3 shows that the solid/liquid interface travels into the bulk solid to a maximum depth of approximately 10–12 Å at about 18 $\pm$ 1 ps. For the Lennard–Jones system there was a delay after the end of the pulse before the material started to regrow. The heat conduction of an EAM metal is much greater than for the LJ system [25], as evidenced by the fact that there is no lag between the end of the pulse and the onset of crystal growth. In fact, for the lower fluences in a 4096-atom system, the heat conduction was such that growth commenced 2–3 ps before the end of the pulse. This is an artifact due to the size of the system. It should be remembered that a system size of 4096 atoms was found to be adequate for studies of LJ systems, but not, it appears, for some aspects of resolidification studies in EAM metals.

The interface temperature versus time curve for a pulse of 20 ps and a fluence of 2.03 mJ cm^{-2} is shown in Figure 4. Two features are apparent. Firstly, therre are oscillations present (as indeed can be seen to a smaller extent in the melt depth curve)

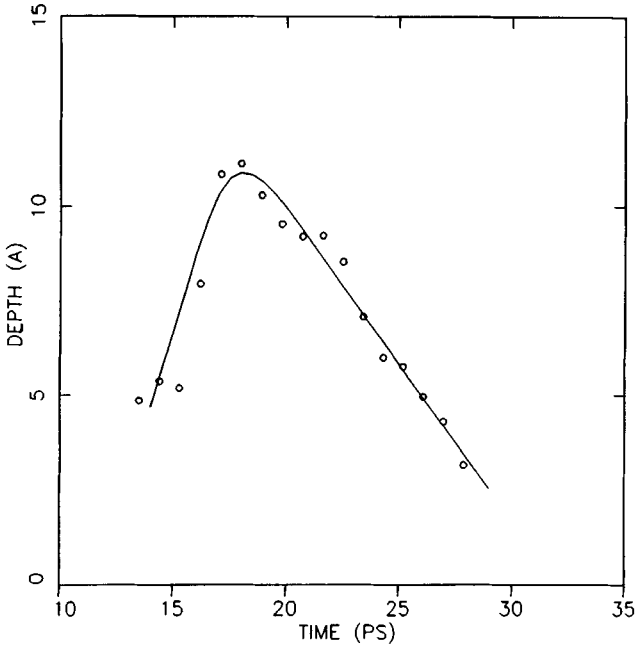

Figure 3 Melt depth versus time for a simulation of 4096 EAM Cu atoms with a substrate temperature of 300 K, a pulse duration of 20 ps, and an absorbed fluence of 2.03 mJ/cm^2. Circles are raw data, solid line represents a best fit to the data

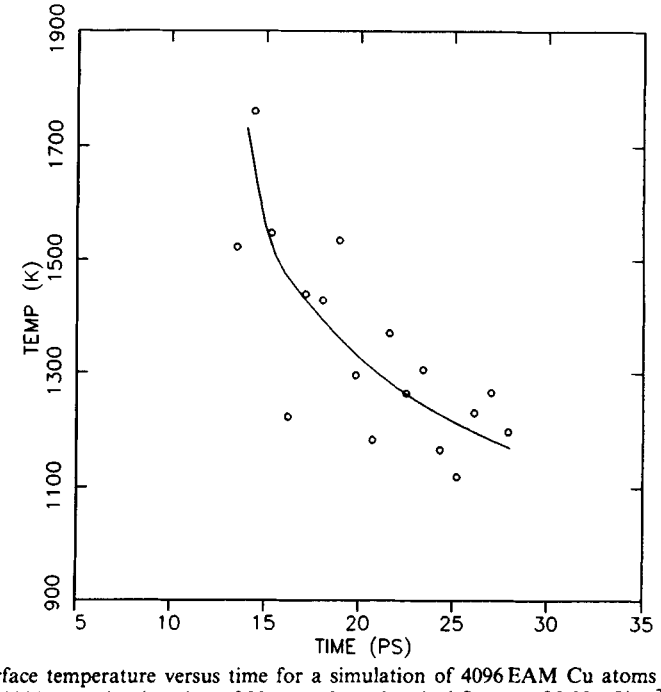

Figure 4 Interface temperature versus time for a simulation of 4096 EAM Cu atoms with a substrate temperature of 300 K, a pulse duration of 20 ps, and an absorbed fluence of 2.03 mJ/cm^2. Circles are raw data, solid line is a best fit to the data.

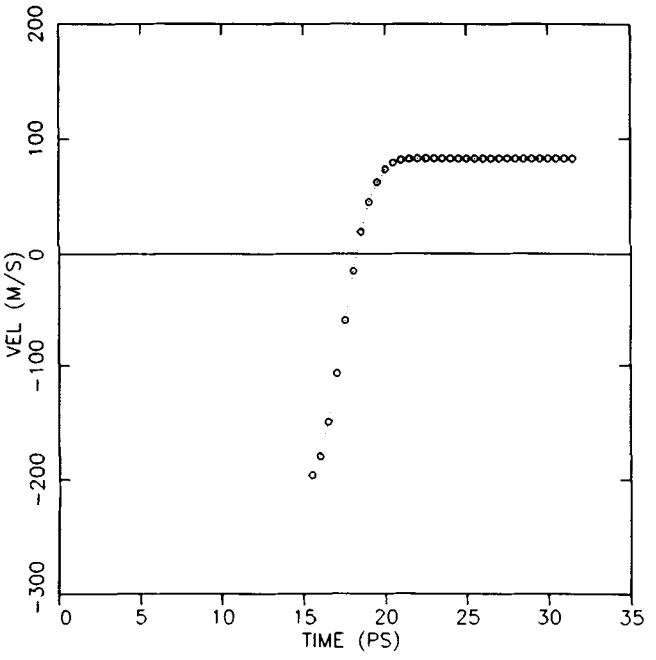

Figure 5 Velocity of the solid-liquid interface versus time for a simulation of 4096 EAM Cu atoms with a substrate temperature of 300 K, a pulse duration of 20 ps, and an absorbed fluence of 2.03 mJ/cm^2. Circles are raw data, dotted line represents a best fit to the data.

and secondly, the period of constant undercooling is very small. In fact, for lower fluences the constant undercooling section is essentially non-existent as indicated by the solid line in Figure 4. The oscillations can be partly attributed to the following phenomenon: when the solid is heated it expands. Due to the static layers at the bottom of the simulation cell there is a net momentum in the z-direction. The expansion continues until it is overcome by the tension in the solid whereupon it starts to contract. The contraction continues past the equilibrium position and the expansion is reinstated. The interface temperature drops during the expansion and rises during contraction. The oscillations in the interface temperature curves can also be partly attributed to the oscillations in the melt depth curves. The position of the interface used to calculate the interface temperature comes from the smoothed melt depth curve. So that when the solid expands it is the cooler layers below the true interface that are being used to calculate the temperature and when the solid contracts, it is the warmer layers above the true interface that are being used to calculate the temperature. Verification of the correlation between the height of the liquid/vapor interface and the interface temperature is shown in Figure 7. However, as we showed for a LJ system, even when we compensated for this center-of-mass motion, the temperature oscillations were not eliminated. Thus, while the oscillations are partly an artifact due to the static lattice acting as a "trampolene", there is an instability in the temperature which is largest during the onset of nucleation and growth and which diminishes steadily as the resolidification proceeds.

In Figures 3 and 4, solid lines have been drawn as a best fit through the oscillating curves. For the interface temperature there is considerable error in drawing this curve

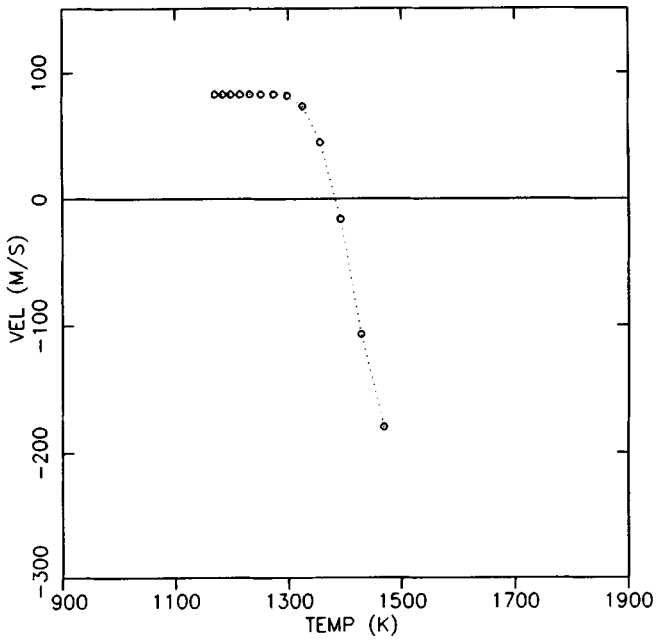

Figure 6 Interface velocity versus interface temperature for a simulation of 4096 EAM Cu atoms with a substrate temperature of 300 K, a pulse duration of 20 ps, and an absorbed fluence of 2.03 mJ/cm^2. Key as for Figure 5.

due to the size of the oscillations. However, the interface velocity-time curve can be calculated from the slope of the melt depth-time plot with little error. Inspection of Figure 5, for example, predicts that there is a period of steady-state regrowth with a velocity of 83 m s^{-1}. The fact that the interface temperature-time curves show such a limited (or absent) region of constant undercooling results in physically-unrealistic interface velocity-interface temperature plots (for example, Figure 6).

In Table 2, we show the steady-state regrowth velocity, v_s, and melting point predicted for the series of energy fluences studied. The melting point is determined from the temperature corresponding to zero velocity in the interface response function. For the 4096-atom system the average melting point for all eight systems is 1357 K with an uncertainty of $\pm$ 60 K. This is excellent agreement with the experimental value of 1358 K. Foiles and Adams [26] calculated the melting point of EAM copper to be 1340 K, but they used the version of EAM parameterized by Foiles, Baskes and Daw [8], whereas we used the older Foiles version [9]. Considering that the EAM parameters were fitted to solid properties, the close comparison between experiment and an EAM model of copper for the melting point is quite an achievement for the potential model. The uncertainty ($\pm$ 60 K) quoted for our "zero velocity" method of calculating T_m is the maximum deviation from the average observed in any of the runs and thus is quite low. Errors in T_m arise from scatter in the melt depth-time plot and from the interface temperature-time curve.

The steady-state resolidification velocity at 300 K for a 20 ps pulse (as in the experiment) ranges from 80 to 109 m s^{-1} for the fluences studied here. The resulting resolidification velocity increases linearly with the absorbed fluence as shown in

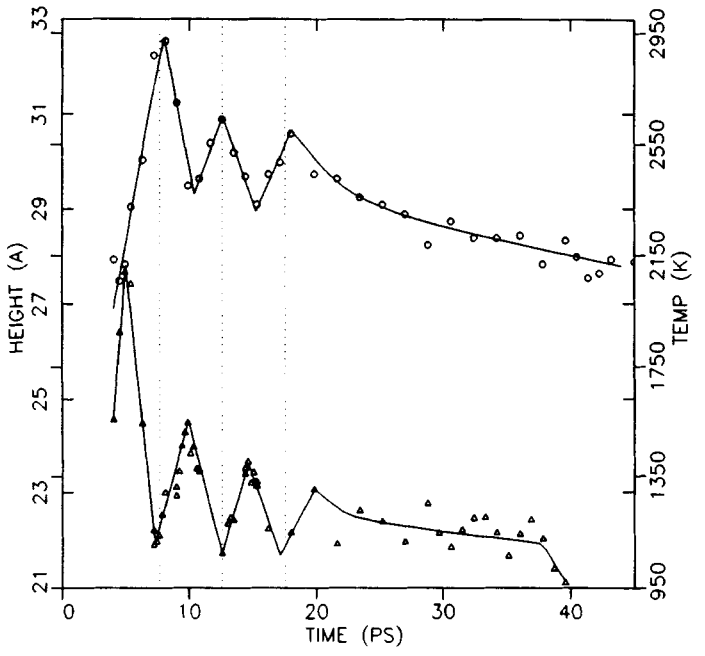

Figure 7 Height of the liquid–vapor interface and temperature versus time for a simulation of 4096 EAM Cu atoms with an absorbed fluence of 3.1 mJ/cm^2 and an 8 ps pulse.
△ = interface temperature
○ = liquid–vapor interface position

Table 2
(a) Copper

System Size/ atoms	*Substrate temperature/K*	*Pulse Duration/ ps*	*Absorbed fluence/mJ cm^{-2}*	*V_s/ m s^{-1}*	*Melting point/K*
4096	300	20	1.86	80.0	1424
4096	300	20	2.03	82.9	1382
4096	300	20	2.45	92.8	1353
4096	300	20	3.20	109.2	1330
8072	300	20	2.19	79.8	1306
8072	300	20	2.63	85.0	1340
4096	300	16	2.90	77.6	1414
4096	300	8	1.95	90.2	1316
4096	300	8	3.10	107.0	1271
4096	710	20	0.82	61.9	1332
4096	1236	20	0.30	9.1	1305
(b) Gold					
4096	300	20	1.10	26	985
4096	220	20	1.06	47	975
4096	220	20	2.06	51	929

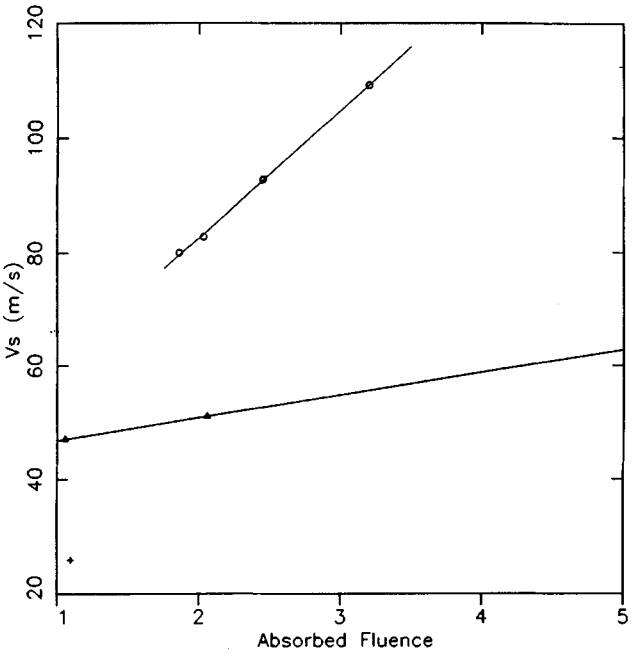

Figure 8 Resolidification velocities for several simulations of copper and gold as a function of the absorbed fluence.
O = 4096 Cu atoms with a substrate temperature of 300 K
x = 8072 Cu atoms with a substrate temperature of 300 K
Δ = 4096 Au atoms with a substrate temperature of 220 K
\+ = 4096 Au atoms with a substrate temperature of 300 K

Figure 8. McDonald *et al.* [2] use a fluence of 23 mJ cm^{-2} in their experiments, but do not quote the value of the fluence absorbed by the copper. These two fluences will be quite different since a lot of the laser energy is lost through reflection. However, for a gold sample irradiated with a fluence of 24 mJ cm^{-2}, they quote the absorbed fluence to be 5 mJ cm^{-2}. The absorbed fluence can be determined by reflectivity measurements and is very sensitive to the wavelength used. Without this information it is difficult for us to ascertain the likely absorbed fluence for copper in McDonald *et al.*'s experiments, but we expect that it has a similar value to that for gold.

We have also studied the effect of changing the pulse duration, by performing simulations with pulses of duration 8 and 16 ps. The results, given in Table 2, show that varying the pulse duration resulted in a different absorbed energy. The resolidification velocities fall within the range obtained for different fluences with 20 ps pulse.

McDonald *et al.* measured the regrowth velocity of copper to be approximately 60 m s^{-1} but they suggest that, due to uncertainties in the time-resolved reflectivity technique used to locate the interface, this value may be only a lower bound. Before we compare our resolidification velocities to experiment we have to redress the unphysical aspects of our simulation, notably the lack of a constant undercooling in the interface temperature during recrystallization. The rapid thermal conduction suggests that for EAM metals there needs to be a greater distancing between the heat

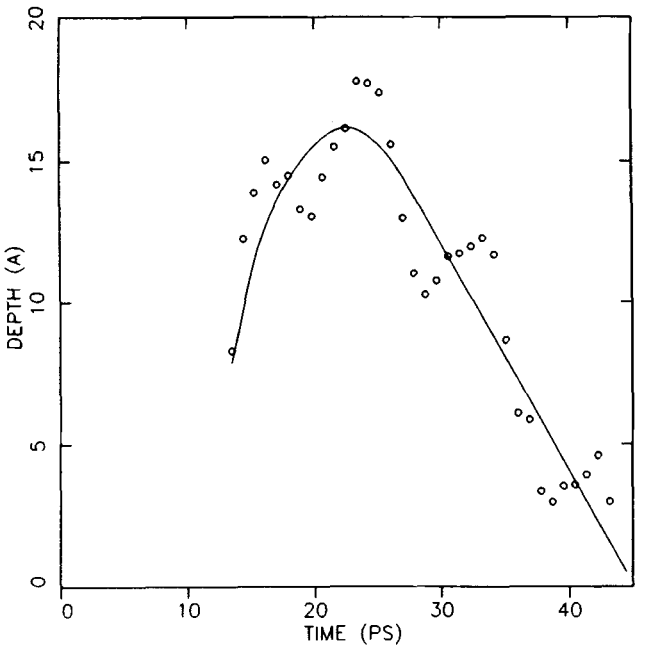

Figure 9 Melt depth versus time for a simulation of 8072 EAM Cu atoms with a substrate temperature of 300 K, a pulse duration of 20 ps, and an absorbed fluence of 2.19 mJ/cm^2.

bath and the transient solid/liquid interface than was necessary for the non-metallic systems we have studied previously.

Effect of system size

In order to test the system size effect we doubled the length of the simulation cell from 30 to 60 layers of solid giving a system size of 8072 atoms. We did not alter the lateral (x-, y-) dimensions from their original values of ~ 29 Å, as some limited testing showed this size to be adequate, though there is always the possibility that long wavelength disturbances arising from the periodic boundary conditions will affect the initialization of melting and regrowth.

The results for the 8072-atom system are shown in Figures 9–11. Notice that the melt depth-time curve (Figure 9) shows much larger oscillations than its counterpart for the smaller system. This is partly due, we suspect, to the dynamic solid "trampolene" region being deeper and partly due to the fact that more data points were calculated for the bigger system allowing the oscillations to be more easily seen. However, there is a considerable improvement in the interface temperature-time curve (see Figure 10). While it still oscillates strongly, it does exhibit a steady-state undercooling during the time period $\sim$ 28–40 ps from the start of the simulation. The undercooling is predicted to be 160 K; no experimental estimate is available. The predicted undercooling is $\sim 11\%$, which is similar to that found in NEMD studies of LJ atoms with similar energy input (a 15 ps pulse of total fluence 25 mJ cm^{-2}) [1].

The velocity of the interface shows a period of steady-state recrystallization with regrowth velocities of 79.8 and 85.0 m s^{-1} for energy fluences of 2.19 and 2.63 mJ cm^{-1}

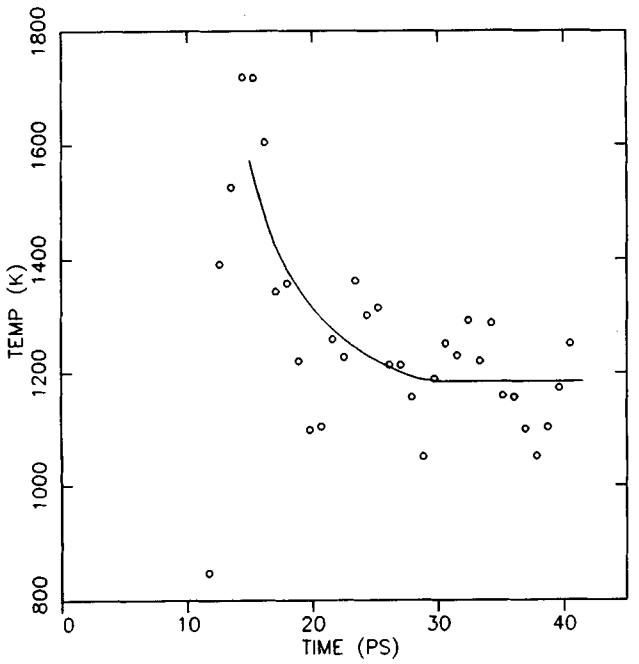

Figure 10 Interface temperature versus time for a simulation of 8072 Cu atoms with a substrate temperature of 300 K, a pulse duration of 20 ps, and an absorbed fluence of 2.19 mJ/cm^2.

respectively. Comparing these to the values for the 4096-atom system, 82.9 and 92.8 m s^{-1} at fluences of 2.03 and 2.45 mJ cm^{-2}, we see that the interface velocity is not unduly affected by the system size. We have already seen that the resolidification velocity increases linearly with fluence, and the results for 4096-atoms show that for absorbed fluences of 1.0–4.0 mJ cm^{-1} the resolidification velocity is predicted by the simulation to lie between 65–130 m s^{-1}. For the larger system, in the same absorbed fluence range, the velocity is predicted to be 65–100 m s^{-1}. The average melting point predicted by simulations of the larger systems is 1323 K (i.e. 2.5% too low); again, in good agreement with experiment.

The constant undercooling produced by the larger system leads to a substantially different interface response function (see Figure 11). The artificial, plateau-like region at large undercooling present in the 4096-atom system is now absent. There is no sign of any asymmetry between melting and freezing kinetics, as evidenced by the constant slope of the velocity–temperature (v–T) curve through the $v = 0$ point. Since the density change on melting is so small for metals we would not expect any asymmetry to occur here. The very slight kink in the curve at around 1420 K is due to difficulties in assigning the velocity close to the maximum in the melt depth-time curve and is not credited with any physical significance.

Effect of the parameterization function

In order to gauge the effect on the kinetics of resolidification of different methods of parameterizing the functions used in the EAM model, we replaced the Foiles *et al.* prescription, which uses Roothaan–Hartree–Fock wave functions for the electron

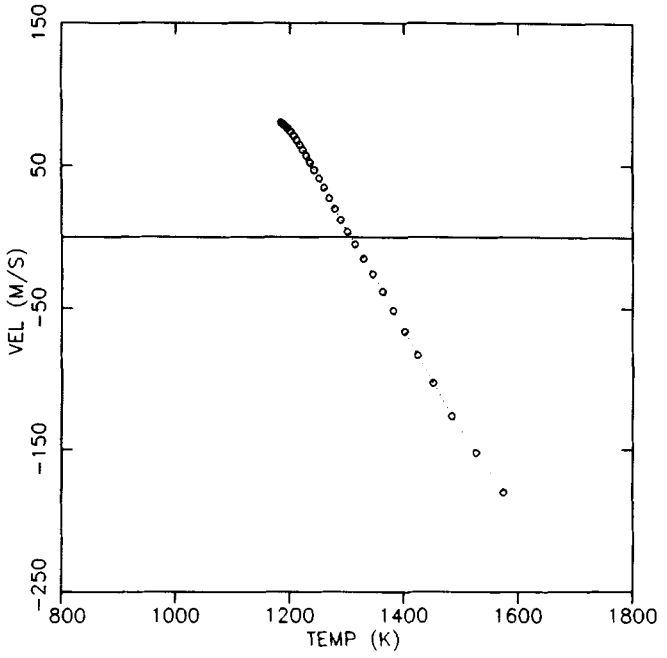

Figure 11 Interface velocity versus interface temperature for a simulation of 8072 Cu atoms with a substrate temperature of 300 K, a pulse duration of 20 ps, and an absorbed fluence of 2.19 mJ/cm^2.

density, by Oh and Johnson's EAM model for copper [11]. Oh and Johnson use simpler exponentially-decaying functions for the electron density. Also, they determine the embedding function by matching the total energy of a perfect crystal to that predicted from an equation of state due to Rose *et al.* [27], whereas Foiles *et al.* use empirically-determined spline knots for the embedding function.

A system of 4096 atoms employing the Oh and Johnson model for copper was equilibrated at 300 K and then irradiated in the same manner as for the Foiles *et al.* model. The melting point determined from the zero velocity point in the interface response function was 1195 K, that is ~ 164 K (or 12%) lower than experiment. There are no startling differences between the results with the Oh and Johnson and Foiles models, although for the Oh and Johnson model there are less oscillations present in both the curves shown in Figure 12 and 13 and the temperature does display a short period of constant undercooling. The undercooling of 140 K is similar to that found for the Foiles *et al.* model for copper. The regrowth velocities for the Oh and Johnson potential were 119 and 80 m s^{-1} for absorbed energy fluences of 2.05 an 2.48 mJ cm^{-2} respectively. It is interesting to note that the regrowth velocity decreases with increasing fluence, whereas it increased with increasing fluence for the Foiles *et al.* model. Experimentally, the velocity increases with increasing fluence before saturating at a certain velocity. The difference in melting point for this model causes the simulation run to be performed at a substrate temperature of $T_{subs}/T_m = 0.25$ rather than the experimental value of 0.22; however this should have a minimal effect on the resolidification velocity.

Higher temperature runs

Simulations of 4096 EAM copper atoms using the Foiles *et al.* parameterization were also carried out where the substrate was held at 710 and 1236 K. These temperatures were chosen in order to compare to results for LJ systems at equivalent fractions of the bulk melting point. The EAM run at 710 K corresponds to 53% of T_m; the closest results for a LJ system was performed at 62% of the melting point [1]. As for the 300 K case, the solid/liquid interface is more diffuse in the LJ system (4 or 5 layers thick) than for EAM copper (3 layers thick). The regrowth velocity at 710 K is $62\,m\,s^{-1}$. This is much faster than the LJ system ($15\,m\,s^{-1}$). This large difference is not surprising due to the more rapid heat conduction in metals (and EAM copper!). The interface temperature-time plot again shows a lot of scatter, with oscillations still present, and there is no period of constant undercooling.

The simulation performed at 1236 K for EAM copper corresponds to a temperature which is 92% of T_m. We have also performed a LJ run at 95% of T_m. The interface morphology differences between EAM and LJ remain the same as for the lower temperatures. The melt depth-time curve at this temperature shows a strange plateau region which we have no reason to believe is a real phenomenon. We have ignored this feature in calculating the interface velocity. The scatter in the interface temperature-time plot for a substrate temperature of 1236 K is very pronounced and, once again, there is no significant region where the undercooling is constant. A very approximate value for the undercooling of 60 K i.e. $\sim 4\%$, is suggested by these results. This smaller undercooling leads to a smaller driving force for resolidification and hence a slower velocity. Due to the strange nature of the melt depth-time curve the steady-state recrystallization velocity, V_s, obtained at this temperature is less accurate than usual, however, we estimate its value to be roughly $9\,m\,s^{-1}$. The corresponding LJ system had a V_s value of $2\,m\,s^{-1}$.

4 RESULTS FOR AN EAM MODEL FOR GOLD

We chose to study gold since, in McDonald *et al.*'s studies at room temperature, the resolidification of gold under pulsed picosecond irradiation was even faster than copper. They report a regrowth velocity of at least $100\,m\,s^{-1}$. Using the Foiles parameterization scheme for gold, we performed an NEMD simulation run for 4096 particles at 300 K with a 20 ps pulse [9] duration and an absorbed energy fluence of $1.10\,mJ\,cm^{-2}$ (cf. experimental values are 20 ps and $5\,mJ\,cm^{-2}$). Qualitatively, the features in the melt depth-time, interface velocity-time and temperature-time plots are similar to those for copper. The interface velocity during the resolidification period was found to be $40\,m\,s^{-1}$. While this is much lower than the experimental value, so is the absorbed energy fluence. However, we found it impossible to impart more than $2\,mJ\,cm^{-2}$ to the system without vaporizing a part of the solid, e.g. approximately 100 of the 4096 atoms vaporized at an absorbed fluence of $2.06\,mJ\,cm^{-2}$. At an absorbed fluence of $2.5\,mJ\,cm^{-2}$, the vaporization of particles from the surface becomes severe, losing ~ 1000 atoms (i.e., 25% of the system!). However, from the three runs performed for gold with absorbed fluences less than $2\,mJ\,cm^{-2}$, we were able to extrapolate our results to the absorbed fluence used in the experiments, as will be described below.

From the zero velocity point in the interface response function, the melting point of EAM gold is given as 980 K, ie. 25% too low. This is in fairly good agreement with Foiles and Adams' free energy calculations which give the value to be 1090 K,

considering that the Au potentials used are not identical. This value was also cross-checked, roughly, by performing an NPT simulation of bulk EAM gold at zero pressure and 1000 K and 1100 K. Though the atoms were placed initially on fcc lattice sites, the resulting phase of the system was that of a liquid suggesting that the apparent melting point is less than 1000 K, in good agreement with the "zero velocity"-derived value of 980 K. Earlier studies of the solid/liquid transition using bulk (surfaceless) NPT simulations have tended to exhibit considerable superheating, up to the limit of mechanical stability. For LJ atoms, the superheating has been shown to be $\sim 15\%$ [28], while for a Stillinger-Weber model of silicon, it is even larger, 30–50% [29]. A Finnis-Sinclair model of copper, which is similar to an EAM model, has been shown [30] to have an apparent melting poing 15% above the *experimental* melting point, but since the melting point of the model is unknown it is not clear to what extent the Finnis-Sinclair model shows any superheating. Holender repeated his calculations [31] in the presence of a solid/vapor interface, where no superheating should occur. In this case the reported T_m is 10% higher than experiment, suggesting a superheating in the surfaceless system of 5%. Our preliminary results suggest that bulk NPT simulations of EAM metals exhibit little or no superheating, in contrast to other previously studied materials. We are currently investigating this more thoroughly.

Since the melting point of EAM gold was found to be lower than experiment, the simulation was run at a T/T_m value of 300./980., i.e. 0.30, whereas the experimental results correspond to a T/T_m value of 0.22. Accordingly, so that a fairer comparison with experiment could be made, we repeated the simulation at a temperature of 220 K (i.e. T/T_m (EAM) = 0.22). The resultant steady-state resolidification velocity of the interface was found to have a slightly larger value, 47 m s^{-1}. Once again, the absorbed energy was only 1.06 mJ cm^{-2}. An additional run at 220 K was performed at an absorbed fluence of 2.06 mJ cm^{-2}. As noted earlier, this simulation suffered a 2% vaporization at the surface. The vaporized atoms did not return to the solid during the simulation. The resolidification velocity was found to be 51 m s^{-1}. From the two runs at 220 K (ie the same T_{subs}/T_m as experiment) we can predict the velocity of regrowth, at 5 mJ cm^{-2}, assuming a linear dependence of v_s with E_{abs} (see Figure 8), to be 63 m s^{-1}. This extrapolation assumes that 5 mJ cm^{-2} is below the energy at which the velocity "saturates", which is a reasonable assumption for a 20 ps laser pulse.

6 DISCUSSION

(i) The melting points of EAM metals have been determined using the zero-velocity point in the interface response function. This method shows that the melting point of copper is 1350 K which is close to experiment (1358 K). The melting point of gold is much too low. A value of 980 K was calculated, which is 25% lower than experiment, but in reasonably good agreement with Foiles and Adams free energy calculations which gave a value of 1090 K using a slightly different set of parameters for gold.

(ii) At 300 K, the steady-state resolidification velocity, v_s, for EAM Cu ranges from 83–100 m s^{-1} for absorbed fluences of approximately 2–5 mJ/cm^2. The experimental value is above 60 m s^{-1} for an unknown absorbed fluence. The simulation results predict an undercooling of 160 K, for which there are no corresponding experimental results.

(iii) At 220 K the regrowth velocity v_s for EAM Au ranges between 47–51 m s^{-1} for absorbed fluences of 1.06–2.06 mJ/cm^2. Extrapolation to the experimental fluence of 5 mJ/cm^2 predicts a value of 63 m s^{-1}. The simulation appears to underestimate the regrowth velocity by a factor of two. However, EAM models ignore the free electron contribution, which dominates the phonon contribution for metals. We are investigating the combined roles of the thermal conductivity and temperature gradients in the simulation. Preliminary results show that these two quantities counterbalance each other and that the underestimated thermal conductivity of EAM gold is largely to blame for the low regrowth velocity for this metal. This study will be the subject of a subsequent publication.

(iv) Surface melting of metals. EAM models of both copper and gold exhibit a disordering of the structure of the crystal/vapor interface at temperatures $> 90\%$ of T_m. The extent of the surface melting for EAM metals is considerably greater than that for non-metals at comparable conditions. At 92% of T_m a Lennard-Jones system would exhibit only one disordered layer: the EAM systems show three or four disordered layers. In addition, it appears that adatom-induced surface reconstruction was observed for a 0.5 monolayer coverage for EAM copper.

(v) Simulation-related details.
Due to the greater heat transfer characteristics of the model, a larger system size is required ($4096 < N < 8072$) for the system to achieve a constant undercooling. In our simulations we emphasized distancing the transient solid/liquid interface from the heat bath by configuring the larger simulation cell to be twice as deep as the smaller system with the same x- and y- dimensions. Strong oscillations were observed in the interfacial temperature for all the simulations. Less pronounced oscillations were observed in Lennard–Jones systems. Smaller systems (4096 atoms) did not sustain a constant undercooling during resolidification. Fortunately, the value predicted for v_s is not affected much by system size. Nor did it seem to be affected by the lack of constancy in the interfacial temperature for the 4096-atom system.

Acknowledgments

We are pleased to acknowledge an AT&T/COMEPP Manufacturing Engineering Fellowship and a Shell Fellowship for CFR. Extensive amounts of computer time on the IBM 3090-600 J machines was provided by the Center for Theory and Simulation in Science and Engineering at Cornell University, which is funded in part by the National Science Foundation, New York State and the IBM Corporation and members of the Corporate Research Institute.

References

[1] D.K. Chokappa, S.J. Cook and P. Clancy, "Non-Equilibrium Simulation Method for the Study of Directed Thermal Processing." *Phys. Rev. B*, **39**, 10075–10087 (1989).
[2] C.A. McDonald, A.M. Malvezzi and F. Spaepen, "Picosecond Time-Resolved Measurements of Crystallization in Noble Metals" *J. Appl. Phys.*, **65**, 129–136
[3] G.H. Gilmer and M. Grabow, "Atomic Scale Calculations in Material Science", *Mat. Res. Soc. Symp. Proc.*, **141**, 349–411 (1989).

[4] J.Y. Tsao, M.J. Aziz, M.O. Thompson and P.S. Peercy, "Asymmetric Melting and Freezing Kinetics in Silicon." *Phys. Rev. Lett.*, **56,** 27112–2715 (1986).
[5] S.M. Foiles, "Embedded Atom Method Studies of Metals." *J. Vac. Sci. and Technol.*,**A4,** 761–763 (1986).
[6] C.F. Richardson and P. Clancy, "Non-Equilibrium Molecular Dynamics Simulation of the Rapid Solidification of Metals." *Mat. Res. Soc. Symp. Proc.*, **159,** 331–335 (1990).
[7] M.S. Daw and M.I. Baskes, "Embedded-atom method: Derivation and application to impurities, surfaces and other defects in metals." *Phys. Rev. Lett.*, **50,** 1285–1288 (1983); *Phys. Rev. B*, **29,** 6443–6453 (1984).
[8] S.M. Foiles, M.I. Baskes and M.S. Daw, "Embedded-atom-method functions for the fcc metals Cu, Ag, Au, Ni, Pd, Pt, and their alloys." *Phys. Rev. B*, **33,** 7983–7991 (1986).
[9] S.M. Foiles, "Application of the embedded-atom method to liquid transition metals." *Phys. Rev. B*, **32,** 3409–3415 (1985).
[10] M.W. Finnis and J.E. Sinclair, "A simple empirical N-body potential for transition metals." *Philos. Mag. A*, **50,** 45–55 (1984).
[11] D.J. Oh and R.A. Johnson, "Simple Embedded Atom Method model for fcc and hcp metals." *J. Mater. Res.*, **3,** 471–478 (1988).
[12] R.A. Johnson and D.J. Oh, "Analytic embedded atom method model for bcc metals." *J. Mater. Res.*, **4,** 1195–1201 (1989).
[13] R.A. Johnson, "Alloy models with the embedded-atom method." *Phys. Rev. B*, **39,** 12554–12559 (1989).
[14] S.J. Cook and P. Clancy, "Solute trapping at a rapidly-moving solid/liquid interface for a Lennard-Jones alloy." *Molecular Simulation*, **5,** 99–117 (1990).
[15] P. Haberle and T. Gustafsson, "Medium-energy ion-scattering analysis of the c(2 × 2) structure induced by K on Au(110)." *Phys. Rev. B*, **40,** 8218–8224 (1989).
[16] S.J. Cook and P. Clancy, unpublished results.
[17] J.W.M. Frenken and J.F. van der Veen, "Observation of Surface Melting." *Phys. Rev. Lett.*, **54,** 134–137 (1985); J.W.M. Frenken, P.M. Maree and J.F. van der Veen, "Observations of Surface Melting." *Phys. Rev. B*, **34,** 7506–7516 (1986).
[18] R.H. Willens, A. Kornblit, J.R., Testardi and S. Nakahara, "Melting of Pb as it approaches a two-dimensional solid." *Phys. Rev. B*, **25,** 290–296 (1982); G. Deraud and R.. Willens, "Observation of the melting transition in thin lead films." *Phys. Rev. Lett.*, **57,** 2683–2689 (1986).
[19] D.M. Zhu and J.G. Dash, "Surface melting of neon and argon films: profile of the crystal-melt interface." *Phys. Rev. Lett.*, **60,** 432–435 (1988).
[20] Helium-atom scattering: U. Harten, A.M. Lahee, J.P. Toennies and Ch. Woll, "Observation of a Soliton Reconstruction of Au(111) by high resolution helium atom diffraction." *Phys. Rev. Lett.*, **54,** 2619–2622 (1985). TEM: K. Takayanagi and K. Yagi, "High Level Electron Microscopy of Metal Surfaces." *Jpn. Inst. Met.*, **24,** 337–348 (1983).
[21] F. Ercolessi, M. Parrinello and M. Tosatti, "Au(100) Reconstruction in the Glue Model." *Surf. Sci.*, **177,** 314–328 (1986); M. Garofalo, E. Tosatti and F. Ercolessi, "Structure Energetics and low Temperature Behavior of the Au(110) Reconstructed Surface." *Surf. Sci.*, **188,** 321–326 (1986).
[22] F. Ercolessi, A. Bartolini, M. Garofalo, M. Parrinello and E. Tosatti, "Au Surface Reconstructions in the Glue Model." *Surf. Sci.*, **189/190,** 636–640 (1987); P. Carnevalli, F. Ercolessi and E. Tosatti, "Surface Melting Behavior of Au(111)." *Surf. Sci.*, **189/190,** 645–648 (1987).
[23] F. Ercolessi, E. Tosatti and M. Parrinello, "Au(100) Surface Reconstruction." *Phys. Rev. Lett.*, **57,** 719–722 (1986).
[24] E.T. Chen, R.N. Barnett and U. Landman, "Crystal-melt and melt-vapor interfaces of nickel." *Phys. Rev. B*, **40,** 924–932 (1989).
[25] Our estimate, from simulations of systems of both EAM Copper and Lennard-Jones atoms, is that the thermal conductivity of EAM copper is 18 times that of a Lennard-Jones system.
[26] S.M. Foiles and J.B. Adams, "Thermodynamic properties of fcc transition metals as calculated with the embedded-atom method." *Phys. Rev. B*, **40,** 5909–5915 (1989).
[27] J.H. Rose, J.R. Smith, F. Guinea, and J. Ferrante, "Universal features of the equation of state of metals." *Phys. Rev. B*, **59,** 2963–2969 (1984).
[28] D.K. Chokappa and P. Clancy, "A computer simulation study of the melting and freezing properties of a system of Lennard-Jones particles. I. Melting the Solid II. Cooling the Liquid." *Mol. Phys.*, **61,** 617–634 (1987).
[29] J.Q. Broughton and X. Li, "Phase diagram of silicon by molecular dynamics." *Phys. Rev. B*, **35,** 9120–9127 (1987).

[30] J.M. Holender, "Molecular dynamics studies of solid and liquid copper using the Finnis-Sinclair many-body potential." *J. Phys: Condens. Matter*, **2,** 1291–1300 (1990).
[31] J.M. Holdender, *Private Communication* (1990).
[32] J.Q. Broughton, G.H. Gilmer and K.A. Jackson, "Crystallization Rates of a Lennard-Jones Liquid." *Phys. Rev. Lett.*, **49,** 1496–1500 (1982).